



PROBABILISTIC DEMAND AND CAPACITY ANALYSIS OF 3-D STEEL FRAMES UNDER SEISMIC EXCITATIONS

K.W. Liao¹, Y.K. Wen²

SUMMARY

The purpose of this study is to develop a method for probabilistic demand and capacity evaluation of 3-D steel moment frames under seismic excitations. Important system demand and capacity contributing factors are investigated such as uncertainty in member properties, randomness of ground motions, and inelastic structural member behaviors including connection brittle failure. Both inherent variability and modeling error are considered. The variability in material properties and member capacity is taken into account by Monte-Carlo simulation. A 3-D finite element model based on ABAQUS is developed, in which the Bouc-Wen smooth hysteresis model is used to describe inelastic and deteriorating restoring force behaviors observed in recent tests of structural members and brittle beam-to-column connections. The system demand is determined by performing time history response analyses of the building under a suite of FEMA/SAC uniform hazard ground motions. The system capacity in terms of the drift ratio against incipient collapse is generally difficult to predict since the structural response goes into nonlinear range before collapse. In this study it is determined by performing an Incremental Dynamic Analysis (IDA). Numerical examples are given. To include modeling errors in the structural demand analysis, a correction factor is applied to the median response. The probabilistic demand and capacity of 3-D steel moment frames are obtained and the effects of the above important factors on the demand/capacity are investigated. Impact on structural reliability, performance, and redundancy is also mentioned.

INTRODUCTION

One of the important issues in performance-based earthquake engineering is evaluation of the probability of a specific performance objectives not being met (e.g. collapse prevention). The ground motion intensity, displacement and force demand, and capacity of buildings are the three primary random elements that one has to consider in the evaluation. In the past, researchers used peak ground acceleration (PGA) to describe the seismic intensity. More recently, the intensity is described in terms of the spectral acceleration (S_a) at the fundamental period of buildings. In view of the large variability of seismic events and ground motions at a given site, the intensity needs to be described in probabilistic forms. The hazard function, $H(S_a)$, describing the probability of seismic intensity, is commonly provided by earth scientists. The structural engineers' major task is then to accurately estimate the response demand and capacity of

¹ Graduate student, Department of Civil Engineering, University of Illinois, USA, kliao@uiuc.edu

² Professor, Department of Civil Engineering, University of Illinois, USA, y-wen@uiuc.edu

buildings under ground motions corresponding to a given probability level. Since structures generally go into inelastic range under severe seismic excitations, the accuracy of the demand and capacity analysis depends largely on the modeling of buildings. In this study, important system demand and capacity contributing factors are investigated, namely, uncertainty in material properties and members, randomness in ground motions, and inelastic structural member behaviors including brittle connection failure.

A commonly accepted practice in seismic designs is to take advantage of the ductility capacity of the system. A ductile system can withstand intense ground excitation without collapse. Before Northridge earthquake, connections of steel moment frames were thought to have the ductility capability. After the earthquake, many brittle connection failures were found and such connections are no longer acceptable. In the ensuing SAC research project, a wide range of bolted beam-column connections, welded-beam-column connections, welded-bolted beam-column connections, and other alternatives have been investigated and reported in FEMA 355D [1], and FEMA 289 [2]. One of the central themes in these reports is determination of the rotational capacity of pre- and post-Northridge connections. The rotational capacity, as expected, was found to be highly random and therefore needs to be carefully considered in the analysis. The Bouc-Wen smooth hysteresis model introduced by Wen [3] has been widely used for inelastic systems because of its capability of modeling a large variety of nonlinear behaviors and computational efficiency as shown in Baber and Noori [4] and Wang and Wen [5]. This model is therefore used herein to evaluate the response demand and capacity of buildings, incorporating the inelastic moment-rotation relationships of connections and their uncertainties documented in the FEMA/SAC and other projects [1, 2]

A building with a regular, symmetric configuration and uniform mass distribution may be modeled as a 2-D frame structure without losing much of accuracy. For buildings with non-uniform mass distribution or with fractured beam-column connections, the biaxial interaction of buildings may have significant effects on the response of buildings under seismic excitation. For this reason, a 3-D finite element model based on ABAQUS is developed to take the biaxial interaction of buildings into consideration. In addition, the gravity frames are also included in the 3-D model; therefore, their effects on the building performance can be investigated more accurately than a 2-D model. The beam column connections of the gravity frames are assumed to be simple hinges in this study following Yun [6].

Structural reliability can be determined in terms of demand versus capacity. In this study, the column drift ratio is used to measure both demand and capacity, i.e. maximum column drift ratio (MCDR) under earthquake ground motion versus the structural capacity against drift. Uncertainty in demand and capacity may be due to inherent variability and modeling errors, also known as aleatory and epistemic uncertainties. Both uncertainties are considered. The displacement demand (D_d) is determined by performing a suite of time history analyses of the response under FEMA/SAC ground motions [7]. The displacement capacity (D_c) is determined by performing an Incremental Dynamic Analysis (Vamvatsikos and Cornell [8]). Since the results of IDA is highly dependent on the record, to evaluate the capacity uncertainty, 3-D IDA studies of the same building under different ground motions are carried out in which the aleatory uncertainties in ground motions, connections, and material properties are also included. Based on the statistics of displacement demand and capacity, the limit state probability, fragility curve, and structural reliability/redundancy analysis are carried out. Wang and Wen [9] proposed a uniform-risk redundancy factor, R_R , to achieve a uniform reliability level for buildings of different redundancies. This factor is used here to evaluate the redundancy of a structure system.

MODELING OF BUILDINGS

Modeling of connections of steel moment frame

Bouc-Wen smooth hysteresis model

Consider a single-degree-of-freedom inelastic system of mass m , damping c , and initial elastic stiffness k , subjected to a ground acceleration $\ddot{u}_g(t)$. The equation of motion of this system can be written as

$$m\ddot{u} + c\dot{u} + q(u, z) = -m\ddot{u}_g(t) \quad (1)$$

in which the total restoring force $q(u, z)$ can be decomposed into an elastic and a displacement time-histroy-dependent inelastic component

$$q(u, z) = \alpha ku + (1 - \alpha)kz \quad (2)$$

where u is the displacement of the system; α is the post-to-pre-yielding stiffness ratio. Based on the Bouc-Wen smooth hysteresis model, z satisfies the following nonlinear differential equation (Wang and Wen [5]):

$$\dot{z} = \frac{\dot{u}}{\eta} \left[A - v|z|^n (\beta \operatorname{sgn}(\dot{u}z) + \gamma) \right] \quad (3)$$

in which β , γ , and n are parameters controlling the shape of hysteresis; A , η , and v controlling the deterioration of the system. A , η , and v vary with time and are assumed to be functions of dissipated hysteretic energy:

$$\begin{cases} A = A_0 - \delta_A E \\ \eta = \eta_0 + \delta_\eta E \\ v = v_0 + \delta_v E \end{cases} \quad (4)$$

in which A_0 , η_0 , v_0 are initial values and δ_A , δ_η , δ_v are the rates of degradation. E is the normalized dissipated hysteretic energy and calculated as follows:

$$E = \frac{1 - \alpha}{F\Delta} \int_0^t kz\dot{u}dt \quad (5)$$

in which F = the yield force and Δ = yield displacement. To see the effect of above parameters on the ultimate hysteretic displacement, z_u , when z reaches the ultimate value, \dot{z} approaches zero, \dot{u} and z have the same sign. Therefore z_u can be obtained as function of the parameters as follows:

$$A - v|z_u|^n (\beta + \gamma) = 0 \quad (6)$$

$$z_u = \left[\frac{A}{v(\beta + \gamma)} \right]^{\frac{1}{n}} \quad (7)$$

Hysteresis loop pinching can be included by incorporating a time-dependent ‘‘slip-lock’’ element (Baber and Noori [4]). The following function is used in this study as a slip-lock element which is originally proposed by Wang and Wen [5].

$$f(z) = \sqrt{\frac{2}{\pi}} \frac{a}{\sigma} \exp \left\{ -\frac{1}{2} \left[\frac{\operatorname{sgn}(\dot{u}) \frac{z}{z_u} - q}{\sigma} \right]^2 \right\} \quad (8)$$

where the parameter a controls the length of the pinching; σ controls the sharpness of pinching; q controls the ‘‘thickness’’ of pinching area. The following function for a is also recommended by Wang [9]:

$$a = a_0 + \left(\frac{u}{z_u} \right) + \delta_a E \quad (9)$$

where a_0 is the initial length of pinching area; δ_a is the rate of spread of pinching; E is the normalized, dissipated energy as defined above. To describe a smooth hysteresis with strength, stiffness degrading and pinching effect, one can combine the slip-lock element with equation (3) and obtain \dot{z} as

$$\dot{z} = \frac{\dot{u}}{\eta} \left\{ A - v|z|^n [\beta \operatorname{sgn}(\dot{u}z) + \gamma] \right\} h(z) \quad (10)$$

in which

$$h(z) = \frac{1}{1 + \frac{f(z)}{\eta} \left\{ A - v|z|^n [\beta \operatorname{sgn}(\dot{u}z) + \gamma] \right\}} \quad (11)$$

Detailed discussions on the properties of parameters can be found in Baber and Wen [10] and Foliente [11]. Figure 1 depicts examples of Bou-Wen model with strength and stiffness degradation.

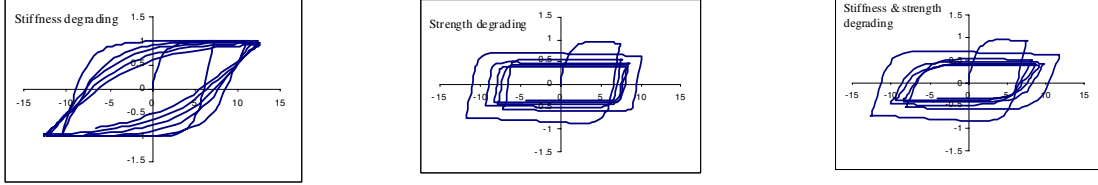


Figure 1. Bou-Wen hysteretic restoring force model with degradation in stiffness (left), strength (center), and both (right).

Development of ABAQUS user-defined-element

ABAQUS [12] allows users to add subroutines to model member behavior. A user-defined-element (UEL) is developed to account for inelastic and degrading connection behavior of steel moment frames in this study. This subroutine is implemented in a 3-D finite element model to investigate the effects of brittle connections on the building performance. The Bouc-Wen model described above is used herein for the ABAQUS UEL. The user subroutine must be coded to describe the contribution of the element to the system model. Depending on static or dynamic analysis, the subroutine must execute various tasks such as defining the contribution of the element to the residual vector (nodal force), defining the contribution of the element to the stiffness matrix, updating the solution-dependent state variables associated with the element (e.g. the plastic energy dissipation), and forming the mass matrix, and so on.

Formulation of an ABAQUS element

The nodal force, F^N , is one of the element's principal contributions to the global system. It depends on nodal variables u^M and on the solution-dependent state variables H^α within the elements. The element load vector can be derived from the potential energy expression shown as follows:

$$F^N = \int_{V_E} [B]^T [E] \{\varepsilon_0\} dV - \int_{V_e} [B]^T \{\sigma_0\} dV + \int_{V_e} [N]^T \{F\} dV + \int_{S_e} [N]^T \{\phi\} dS \quad (12)$$

in which $[E]$ = the material property matrix

$\{\varepsilon_0\}, \{\sigma_0\}$ = initial strains and initial stresses

$\{F\} = [F_x \quad F_y \quad F_z]^T$, body forces

$\{\phi\} = [\phi_x \quad \phi_y \quad \phi_z]^T$, surface tractions

S, V = surface area and volume of the structure

$[N]$ = the shape function matrix

In such cases, external forces will induce positive nodal forces and internal forces will induce negative nodal forces. For step-by-step integration of the equations of motion, a computational method is developed by Hilber and Hughes (1978). It is a modification of Newmark β Method by introducing an additional parameter (α), in which the overall dynamic equilibrium equations is described as follows:

$$F^N = -M^{NM} \ddot{u}^M_{t+\Delta t} + (1 + \alpha)G^N_{t+\Delta t} - \alpha G^N_t \quad (13)$$

in which $M^{NM} = M^{NM}(u^M, \dot{u}^M, H^\alpha, \dots)$ and $G^N = G^N(u^M, \dot{u}^M, H^\alpha, \dots)$; in other words, the largest time derivative of u^M in M^{NM} and G^N is \dot{u}^M , so that

$$-\frac{\partial F^N}{\partial \ddot{u}^M_{t+\Delta t}} = M^{NM}$$

M^{NM} is the nodal mass and G^N is the total force at the degree of freedom N, excluding the inertial forces. Since the Hilber-Hughes time integration scheme is always used in the dynamic analysis in ABAQUS, the element's contribution F^N to the overall residual must be formulated as shown in equation (13).

The element's stiffness contribution to the system model can be obtained from the Hilber-Hughes α method by rearranging the formulation. The acceleration and velocity from Newmark β method are listed as follows:

$$\ddot{u}^M_{t+\Delta t} = \frac{1}{\Delta t^2 \beta} (u^M_{t+\Delta t} - u^M_t) - \frac{1}{\Delta t \beta} \dot{u}^M_t + (1 - \frac{1}{2\beta}) \ddot{u}^M_t \quad (14)$$

$$\dot{u}^M_{t+\Delta t} = \frac{\gamma}{\Delta t \beta} (u^M_{t+\Delta t} - u^M_t) + (1 - \frac{\gamma}{\beta}) \dot{u}^M_t + \Delta t (1 - \frac{\gamma}{2\beta}) \ddot{u}^M_t \quad (15)$$

Substituting equations (14) and (15) to equation (13), one can obtain a generalized force-displacement relationship as follows:

$$K^* u^M_{t+\Delta t} = F^*_{t+\Delta t} \quad (16)$$

in which

$$K^* = \frac{1}{\Delta t^2 \beta} \frac{\partial F^N}{\partial \ddot{u}^M} + \frac{\gamma(1 + \alpha)}{\Delta t \beta} \frac{\partial F^N}{\partial \dot{u}^M} + (1 + \alpha) \frac{\partial F^N}{\partial u^M} \quad (17)$$

Therefore, the element's stiffness contribution to the global stiffness matrix must be formulated as shown in equation (17).

Modeling of Pre-Northridge and Post-Northridge connections

Prediction of connection capacity against fracture is very important due to its significant influence on the building performance. Structural element rotation (or rotational ductility) is commonly used as a damage measure. In addition, the hysteretic energy dissipation also can be a good damage indicator. In the FEMA/SAC project [1, 2], a series of experiments were conducted to investigate the performance of steel moment frame connections, including those of pre-Northridge and post-Northridge connections. The rotational capacity of connections was estimated by a least squares fit to experimental data (FEMA 355D [2]). The plastic rotational capacity at failure, θ_p , is defined as the maximum plastic rotation at which initial fracture occurred or where the resistance dropped below 80% of the plastic moment capacity calculated from the measured yield stress of the steel. For pre-Northridge connections, the focus is on the welded-flange-bolted-web connections. For post-Northridge connections, both bolting and welding connections are considered, and several modifications to improve the performance of connections, such as haunches, cover-plates are also included. Depending on the different types of connections, capacity prediction formulas based on regression analyses of test data are provided. Only pre-Northridge connections with older E70T-4 welds and steels with lower yield tension stress, and post-Northridge connections with reduced beam section (RBS) are considered in this study. The mean value of rotational capacity (θ_p) and standard deviation of θ_p of pre-Northridge connections as function of the beam depth d_b are:

$$\theta_{pmean} = 0.051 - 0.0013d_b \quad (18)$$

$$\sigma_p = 0.0044 + 0.0002d_b \quad (19)$$

The mean value of rotational capacity (θ_p) and standard deviation of θ_p of post-Northridge connections are:

$$\theta_{pmean} = 0.05 - 0.0003d_b \quad (20)$$

$$\sigma_p = 0.02 + 0.0006d_b \quad (21)$$

in which θ_{pmean} and σ_p are in radians, and d_b is in inches.

FEMA 289 [1] provides detailed information of experiments such as connection details, applied loading/displacement histories, and cumulative energy dissipations. The energy dissipation capacity data of the pre- or post-Northridge connection are used in a regression analysis performed in this study assuming that the scatter follows a log-normal distribution and the median value is a linear function of the beam depth. The regression results of the dissipation energy capacity of connections with W30 beam are shown in Figure 4. As in the case of rotational capacity, the depth of beam also has a significant effect on the capacity of dissipation energy. The median value of the dissipation energy capacity (E_d) of pre-Northridge connections is calculated as follows

$$\bar{E}_d = 112.5d_b - 2804 \quad (22)$$

The coefficient of variation δ_{E_d} is assumed to be constant and determined to be 1.19. For post-Northridge connections, the median value is

$$\bar{E}_d = 29.2d_b + 4512 \quad (23)$$

with a δ_{E_d} of 0.39. To reproduce the highly uncertain capacity of connections, the capacities of rotation and dissipation energy of connections are modeled as random variables with parameters given by the above regression results. During the time history analysis, rotation and dissipation energy of connections are calculated at each time step. The fracture of connections occurs when both of them exceed their random capacities, which are simulated via the Monte-Carlo method. In other words, the capacities of connections are different at different locations in the analysis.

Once the fracture of a connection has occurred, a bilinear model is used to describe the post-fracture behavior of this connection with the residual strength of this connection assumed to be maintained at 10% of the yielding strength. A comparison of experimental and analytical behaviors of post-Northridge connections without fracture is shown in Figure 2. Comparison of experimental and analytical behaviors of post-Northridge connections with fracture is shown in Figure 3.

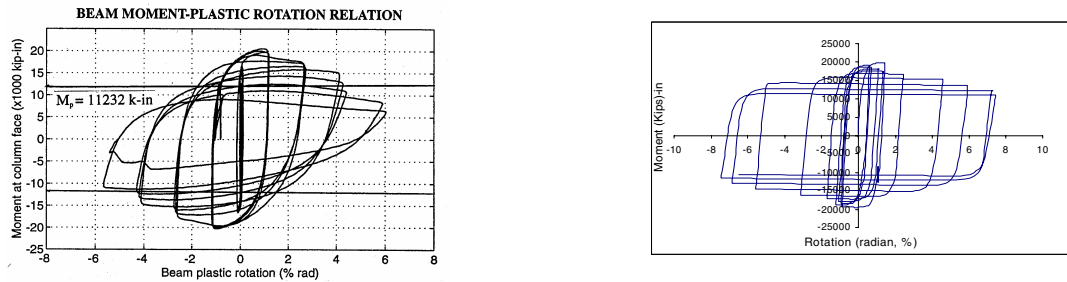


Figure 2. Comparison of experimental (left) and analytical (right) hysteretic behaviors of post-Northridge connection without fracture (FEMA 289 [1]).

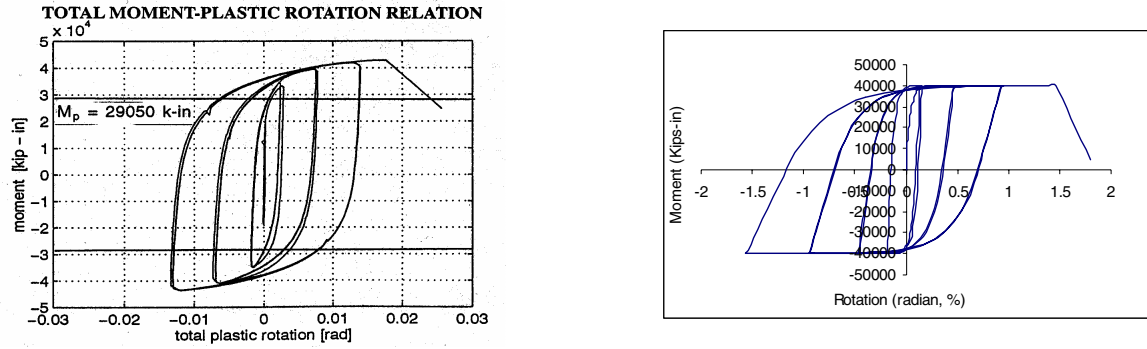


Figure 3. Comparison of experimental (left) and analytical (right) hysteretic behaviors of post-Northridge connection with fracture (FEMA 289 [1]).

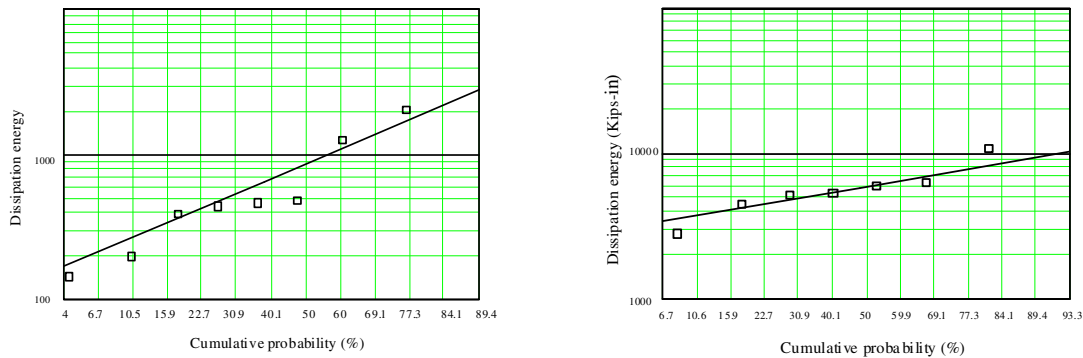


Figure 4. Energy Dissipation of pre-Northridge (left) and post-Northridge buildings (right) plotted on the log-normal probability paper.

Modeling of gravity frames

Lateral resistances of gravity frames are usually ignored in structural response analysis since the beams and columns are only connected at the webs and not at the flanges. Nevertheless, based on the experimental results of Liu and Astaneh-Asl [13], the gravity frames also supply some lateral resistance when there is a compression force in the composite floor slab connected to the beam by shear studs. Yun [6] developed a simple connection model to simulate the gravity frame connections, and the results revealed that although the lateral resistance from gravity frame is significant, most of the contribution is from the flexible deformation of continuous columns connected to the rigid floor slabs and not from the connections. One of the reasons that the connections do not supply much resistance is that the connections lose strength significantly in the very early stages of the loading. Therefore, once the continuous columns of gravity frames are properly modeled, the rotational stiffness of connections of gravity frames can be ignored. Gravity frames is included in finite element models and the connection behavior of gravity frames is assumed as a simple hinge in this study.

UNCERTAINTY TREATMENT AND CAPACITY ANALYSIS

Uncertainty in materials

Material properties of building are inherently random and need to be considered in the structural analyses. In view of the complexity and uncertainty of the nonlinear structure response, a probabilistic treatment is necessary and can be done via Monte-Carlo simulations. The yield strength of Grade 50 steel (F_y) and the elastic modulus of structural members are modeled by normal variables with mean values equal to 50 (ksi) and 29000 (ksi), and coefficients of variation of 15% and 4%, respectively (Kennedy [14]).

Uncertainty in ground motions

FEMA/SAC phase-2 ground motions [7] corresponding to 2% and 10% exceedance probability in 50 years are used in this study. They are compatible with the USGS uniform-hazard target response spectra. Structural time history response is calculated for each of ten uniform-hazard ground motions. The advantage of using such ground motions is that the suite of ten ground motions allows one to evaluate the structural response of a small probability of exceedance that normally required considerably larger number (thousands) of structural response analyses.

Uncertainty Correction Factor for Modeling Errors

To include epistemic uncertainties (modeling errors) in the structural demand analysis, a correction factor is applied to the median response (Wen and Foutch [15]). The correction factor is provided by

$$C_F = 1 + \frac{1}{2} S \delta_Y^2 \quad (24)$$

in which

$$S = \frac{\ln S_{a,m} - \lambda}{\xi^2} \quad (25)$$

$$\delta_Y = [\exp(\sigma_{\ln Y}^2) - 1]^{0.5} \quad (26)$$

$$\sigma_{\ln Y}^2 = \sigma_{\ln D|S}^2 + \sigma_{\ln D}^2 \quad (27)$$

S stands for a sensitivity factor; λ and ξ are the log-normal distribution parameters in the elastic spectral acceleration hazard curve; $S_{a,m}$ is the median system limit state capacity in terms of elastic spectral acceleration; Y is the total uncertainty random variable assumed to be log-normal; δ_Y is the coefficient of variation of Y, related to the variance of $\ln Y$ by equation 26; $\sigma_{\ln Y}^2$ can be obtained by combining the record-to-record response variation for a given elastic spectral acceleration, $\sigma_{\ln D|S}^2$, and the capacity modeling errors, $\sigma_{\ln D_{cao}}^2 \cdot \sigma_{\ln D_{cap}}^2$ is assumed to be 30% in this study.

Incremental Dynamic Analysis

System capacity against the incipient collapse is determined by the Incremental Dynamic Analysis (IDA) (Vamvatsikos and Cornell [8]). A single-record IDA represents a series of dynamic nonlinear analyses of one building under a single ground motion scaled incrementally in terms of its biaxial elastic spectral acceleration. The result is highly dependent on the record chosen; therefore, to fully capture the uncertainty, it is necessary to collect IDA studies of the same building under different ground motions.

The capacity described by each IDA curve, in terms of the drift ratio, is taken at the point when the curve slope is less than 20% of the initial slope [8]. Since the responses go into the highly nonlinear range, the IDA curve could have seriously distorted sections. The capacity of the system is therefore difficult to determine and some judgment may be needed. IDA has been restricted to 2-D plane frame analyses in the past. It is extended to 3-D analyses in this study, in which the aleatory uncertainty in ground motions, connections, and material properties are considered via simulation as described in the earlier section, from which the system capacity against incipient collapse and its uncertainty can be determined.

RELIABILITY AND REDUNDANCY

Structural reliability can be determined in terms of the displacement demand versus capacity. In this study, the maximum column drift ratio (MCDR) is used to measure both demand and capacity. Both aleatory and epistemic uncertainties in the demand and capacity are considered.

The displacement demand (D_d) is determined by performing a suite of time history analyses of the response under the SAC ground motions. In the demand analysis, the MCDR is assumed to follow a log-normal distribution at each hazard level. The median MCDR responses multiplied by the correction factor to include the capacity uncertainty at the two hazard levels (e.g. 10% and 2 % in 50 yrs) then allow one to determine the probabilistic drift demand curve, which has been shown to closely follow a log-normal distribution [9]. The probabilistic drift demand curve is obtained for a building and used to calculate a uniform-risk redundancy factor (R_R , to be defined later) for each building. The displacement capacity (D_C) is determined by performing an IDA [8] as described in the foregoing section.

Limit state probability analysis, fragility curve analysis, and redundancy analysis are carried out using the demand and capacity statistics obtained above. For a given building, the limit state probability can be expressed as follows:

$$P[LS] = \int P[LS|D = d]f_D(d)dd \quad (28)$$

where D is a random variable describing the displacement demand on the system, and $P[LS|D = d]$ is the conditional limit state probability, given $D = d$, or the fragility curve. $f_D(d)$ is the density function of D . The fragility curve is therefore a function of the capacity of the system and its uncertainty.

Wang and Wen [9] proposed a uniform-risk redundancy factor, R_R , for design to achieve a uniform reliability level for buildings of different redundancies. This factor can be also used to evaluate the redundancy of a given structural system. The R_R factor is defined as follows:

$$R_R = \begin{cases} 1 & \text{when } P_{ic} \leq P_{ic}^{all} \\ \frac{S_a^{ic}}{S_a^{all}} & \text{when } P_{ic} \geq P_{ic}^{all} \end{cases} \quad (29)$$

where P_{ic} denotes the actual probability of incipient collapse; P_{ic}^{all} denotes the allowable probability of incipient collapse; and S_a^{ic} and S_a^{all} represent the elastic spectral acceleration at the fundamental period causing incipient collapse at these two probability levels. The elastic spectral acceleration at the fundamental period has been used as a seismic hazard intensity measure. This study focuses on 3-D structural response under biaxial excitations in which interaction between responses in the two principal directions and torsional motion are important. Wang and Wen [9] found the biaxial spectral acceleration (BSA) to be a more consistent measure of seismic hazard considering biaxial response. BSA defined as the maximum value of the vector sum of the accelerations in the two orthogonal directions throughout time history analysis, is then used in this study. The target (allowable) probability of incipient collapse is assumed to be 2 % in 50 years. The required design force is multiplied by a factor of $1/R_R$ to achieve the same reliability against incipient collapse for buildings of different reliability/redundancies.

NUMERICAL EXAMPLE

Building Design

One building is designed according to a current code and its capacities against rotation, energy dissipation and incipient collapse are randomized as described in the foregoing sections to investigate the effects of these uncertainties on the building performance. The building is square in plan configuration with width and length of 150 ft. It has three stories with a story height of 13 feet. There are five bays in each direction. Only center three bays of the perimeter frames are designed as moment frames and the rest are gravity frames (Figure 5). Both pre-Northridge and post-Northridge connections are considered in the moment frames.

Design Assumptions

The design of the frame follows the 2000 International Building Code and the 1997 AISC Seismic Provisions. Design assumptions for special moment resisting frames are:

1. Strong column weak beam (SCWB) guideline is used, i. e. the sum of the moments in the column above and below the joint at the intersection of beam and column centerlines should be no less than the sum of the moments in the beams at the intersection of beam and column centerlines [16, 17].
2. 5% damping in first and second modes is used in time history analysis.
3. The floors are modeled as flexible diaphragms. The SCWB design guideline is used here. It prevents plastic hinges in the columns. Notice that, a rigid diaphragm can cause plastic hinges in the columns. In addition, to consider the effects of fracture of beam/column connections, beams and floors should remain as flexible to allow the development of such fracture failures.
4. The buildings are located in Los Angeles, California. The site class is assumed to be type D. Seismic Use Group I is assigned to the building. As a result, the seismic response coefficient (C_s) is calculated by the follows:

$$C_s = \frac{S_{DL}}{\left(\frac{R}{I_E}\right)^* T} \quad (30)$$

in which S_{DL} (= 0.81g) is the design hazard, R (= 8) is the response modification factor, I_E (= 1) is the occupancy importance factor, and T (= 0.55 second) is the fundamental period estimated by $0.035 \times (H)^{0.75}$. H is the height of building (ft).

The assumptions above lead to beam sizes controlled by the strength requirement instead of drift criteria, and the column sizes are controlled by the SCWB guideline. The member sizes of moment frames and gravity frames of this building are shown in table 1.

Table 1. Detailed design of a 3-story building.

	1F		2F		3F	
	beam	Column	beam	column	beam	Column
Gravity frames	W24X207	W14X193	W24X207	W14X193	W24X162	W14X145
Moment frames	W24X279	W14X550	W24X279	W14X550	W24X207	W14X455

Results of analyses

The finite element model of this building is shown in Figure 5, in which the bold lines represent the moment frames. Examples of pre- and post-Northridge connection hysteretic behaviors of this building are shown in Figure 6. The fundamental period of this building is 0.6 second and the results of analyses will be described in the following sections.

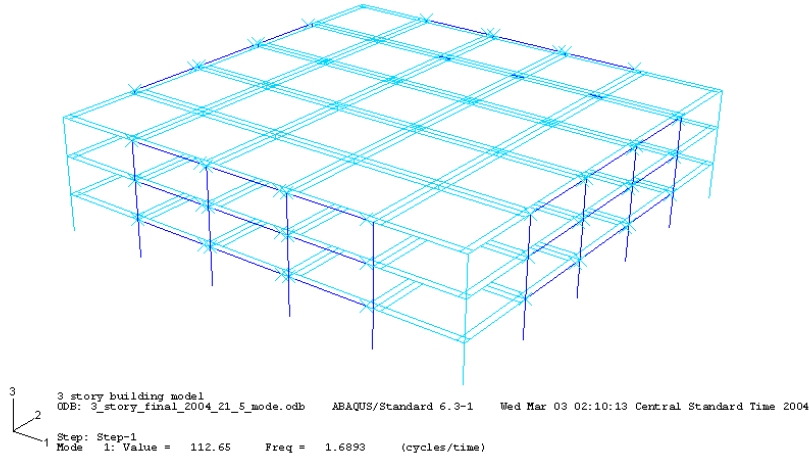


Figure 5. Finite element model of a 3-D building.

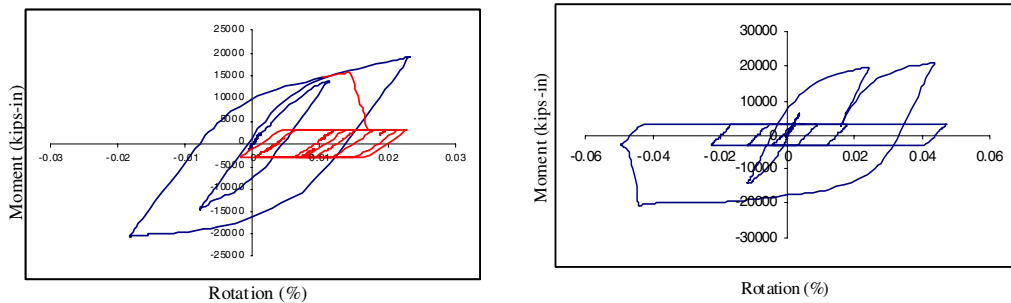


Figure 6. Pre-Northridge (left) and post-Northridge (right) connection hysteretic behaviors of the demonstrated building.

Results of demand and capacity analyses

The probabilistic drift demand curve is determined by multiplying the median MCDR determined from the time history analyses with the correction factors at the two hazard levels. The displacement capacity (D_C) against incipient collapse is determined by performing IDA as described in the foregoing section. Table 2 and Figure 7 show the results of demand analysis. As expected, fracture failure of the pre-Northridge connections has a serious impact on the building performance. For the 2% in 50 years hazard, the median drift demand of pre-Northridge buildings is almost twice that of the post-Northridge buildings.

Figure 8 shows the results of IDA analysis of the buildings with pre- and post-Northridge connections. For each set of IDA curves, building properties are randomized. The incipient collapse capacity can be established from the IDA analysis and approximately described by a lognormal distribution as shown in Figure 9. Table 3 shows the statistics of drift capacities for the two buildings. As one can see that the capacity of the pre-Northridge building is only 60% of the post-Northridge building. To examine the history of fracture development throughout an IDA analysis, Figure 10 shows the fraction of the number of fractured connections to the total number of connections in a selected IDA curve, in which the ground motions LA27 and LA28 are used. The result indicates that the significant fracture behavior starts at about BSA at 2.5g corresponding to the 2/50 level (eight of seventy-two connections are fractured). The system is near the overall collapse stage at 1.4 times 2/50 BSA (sixty-two of seventy-two connections are fractured).

Table 2. Median and coefficient of variation(C.O.V.) of maximum column drift ratio (MCDR) of the building at two hazard levels.

Hazard level		10/50		2/50	
Connection type		Median (%)	c.o.v.	Median (%)	c.o.v.
3-story	pre-Northridge	2.38	0.57	4.7	0.70
3-story	post-Northridge	1.48	0.33	2.47	0.32

Table 3. Statistics of drift capacity against incipient collapse of pre-Northridge and post-Northridge buildings.

Connection type	Median (%)	c.o.v.
pre-Northridge	5.5	0.46
post-Northridge	8.9	0.25

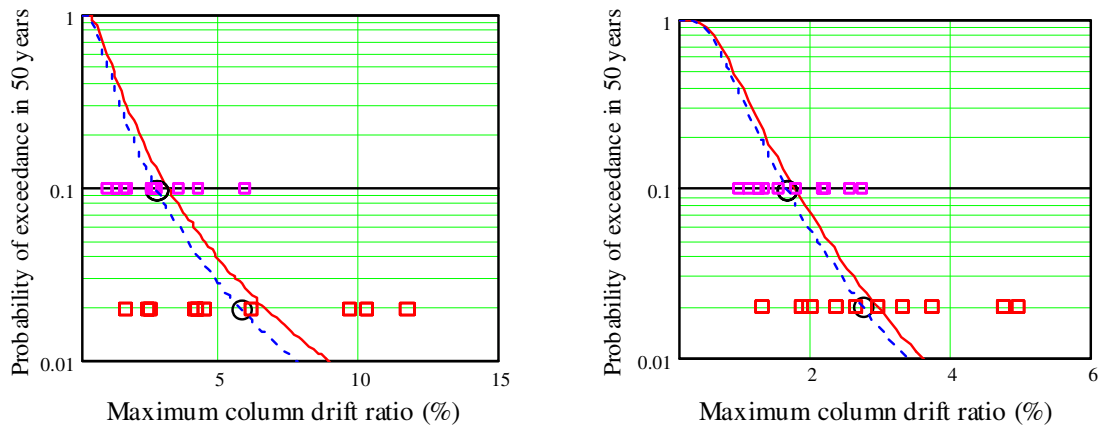


Figure 7. Probabilistic MCDR demand curve of 3-story building at LA, CA. with pre-Northridge connections (left) and post-Northridge connections (right) are shown. Solid and dashed lines indicate performance curve with and without consideration of epistemic uncertainty. O indicates the median value.

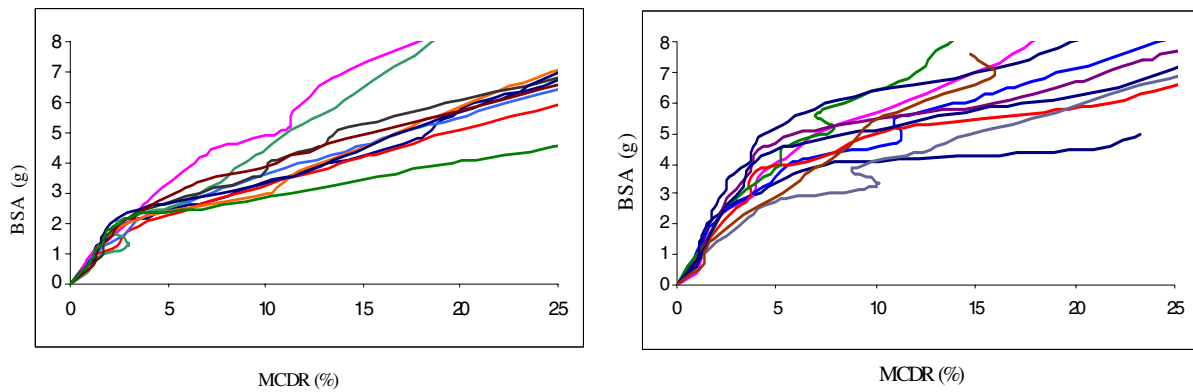


Figure 8. IDA curves of pre-Northridge (left) and post-Northridge (right) buildings.

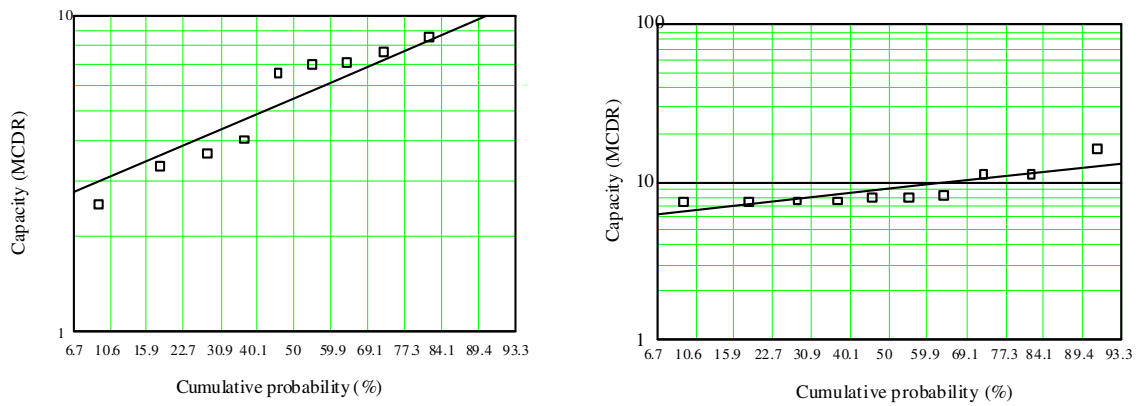


Figure 9. Building drift (%) capacity against incipient collapse with pre-Northridge (left) and post-Northridge (right) connections plotted on the log-normal probability paper.

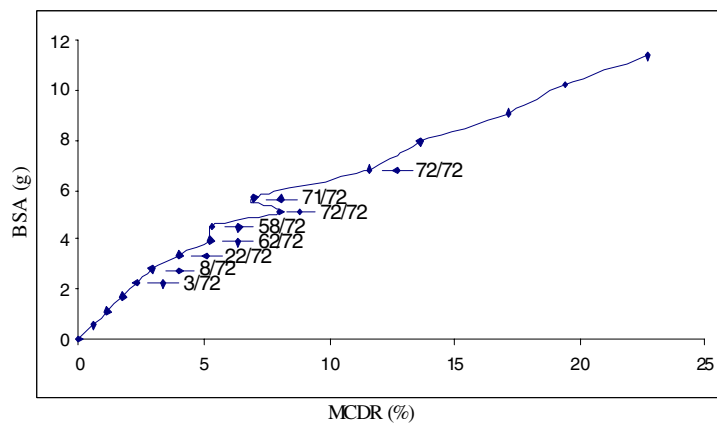


Figure 10. IDA curve under two SAC ground motions , LA27 and LA28.

Results of reliability analysis

Based on the formulas shown in the foregoing, the 50-yr limit state probability, fragility curve and redundancy factor (R_R) are calculated. The results are shown in Table 4, Figure 11, and Table 5, respectively. The drift ratio thresholds for limit state of Immediate Occupancy (IO), Life Safety (LS), and Collapse Prevention (CP) are based on recommendation of FEMA 273. That for Incipient Collapse is determined from the IDA analysis as shown above. It is seen that the pre-Northridge building has considerably higher failure probability in each performance categories and is more vulnerable due to the earlier fracture of connections. Also the R_R for the pre-Northridge building is 0.879 indicating a lack of reliability/redundancy. It needs to be strengthened to bring this factor up to 1.0 to achieve the desired reliability level of 2% in 50 years against incipient collapse.

Table 4. 50-yr limit state probability building with pre-Northridge and post-Northridge connections.

Connection type	Limit state			
	I.O.	L.S.	C.P.	I.C.
pre-Northridge	0.75	0.147	3.8E-2	4.6E-2
post-Northridge	0.687	3.8E-2	3.546E-3	5.9E-4

Table 5. Uniform-risk redundancy factor of pre-Northridge and post-Northridge buildings.

	pre-Northridge	post-Northridge
R_R	0.879	1.0

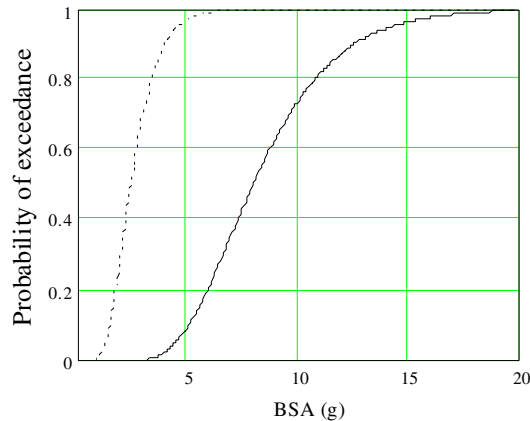


Figure 11. Fragility curves of pre-Northridge (dashed line) and post-Northridge (solid line) buildings.

CONCLUSION

To investigate the probabilistic demand and capacity of steel frame buildings, user-defined-elements are developed and incorporated in ABAQUS. The Bouc-Wen smooth hysteresis model is used to describe the inelastic behavior of connections observed in the experiments. A 3-story steel moment frame building

with pre-Northridge and post-Northridge connections are considered and modeled as 3-D frames. The incremental dynamic analysis (IDA) is also successfully extended to 3-D frames to determine the building capacity against incipient collapse. Based on the statistics of demand and capacity of the building obtained under FEMA/SAC ground motions, analyses of the limit-state probability, fragility, and structural reliability/redundancy, is carried out. The results indicate that the pre-Northridge building has much higher failure probability in all performance categories from immediate occupancy to incipient collapse therefore much more vulnerable to future seismic excitation due to the earlier development of connection fractures. Also it lacks redundancy according to the uniform-risk redundancy factor being less than one. It needs to be strengthened accordingly to achieve the desired reliable level against incipient collapse. The numerical examples demonstrate the capability of the proposed method for application in reliability and performance evaluation and reliability-based design for buildings and structures under seismic excitations.

REFERENCES

1. FEMA-289, "Connection Test Summaries." *Federal Emergency Management Agency*, Washington D. C., 1997.
2. FEMA-355D, "State of Art Report on Connection Performance." *Federal Emergency Management Agency*, Washington D. C., 2000.
3. Wen, Y. K. "Method for Random Vibration of Hysteretic Systems." *Journal of Engineering Mechanics Division, ASCE*, 102, EM2 (April 1976): 249-263.
4. Baber Thomas T. and Noori Mohammad N., "Random Vibration of Degrading, Pinching Systems." *J. Engrg. Mechanics*, 1985, ASCE, 111(8), 1010–1017.
5. Wang, C-H. and Wen, Y. K., "Evaluation of pre-Northridge Low-Rise Steel Buildings—Part I, Modeling." *J. Struct. Engrg.*, 2000, ASCE, 126(10), 1160–1169.
7. Somerville, P., Smith, N., Punyamurthula, S., and Sun, J., "Development of ground motion time histories for phase 2 of the FEMA/SAC steel project." Rep. No. SAC/BD-97/04, Sacramento, Calif., 1997.
6. Yun S. Y., "Performance Prediction and Evaluation of Low Ductility Steel Moment Frames for Seismic Loads." PhD thesis, D. A. Foutch, faculty advisor, Dept. of Civ. and Environ. Engrg, Univ. of Illinois at Urbana-Champaign, Ill., 2000.
8. Vamvatsikos Dimitrios and Cornell C. A., "Incremental Dynamic Analysis." Submitted to *Earthquake Engrg. Struct. Dyn.*, 2002.
9. Wang, C-H. and Wen, Y. K., "Evaluation of pre-Northridge Low-Rise Steel Buildings—Part II, Reliability." *J. Struct. Engrg.*, 2000, ASCE, 126(10), 1169–1176.
10. Baber Thomas T. and Wen Yi-Kwei, "Random Vibration of Hysteretic, Degrading Systems." *J. Engrg. Mechanics*, 1981, ASCE, 107(EM6), 1069–1074.
11. Foliente Greg C., "Hysteresis Modeling of Wood Joints and Structural Systems." *J. Struct. Engrg.*, 1995, ASCE, 121(6), 1013–1017.
12. ABAQUS version 6.4 online documentation, 2003.
13. Liu, J. and Astaneh-Ael, A., "Cyclic Tests on Simple Connections Including Effects of the Slab." SAC Report No. SAC/BD-00/03, 2000.
14. Kennedy D. J. L. and Baker K. A., "Resistance Factors for Steel Highway Bridges." *Can. J. Civ. Eng.*, Ottawa, 1984, Vol. 11, 324-334.
15. Wen, Y. K. and Foutch, D. A., "Proposed statistical and reliability framework for comparing and evaluating predictive models for evaluation and design critical issues in developing such framework." Rep. No. SAC/BD-97/03, FEMA/SAC Project, Sacramento, Calif., 1997.
16. IBC 2000, "International Building Code." BOCA, ICBO., 1998.
17. AISC, "Seismic Provisions for Structural Steel Buildings." ANSI/AISC 341-02, 2002.